Journal Syifa Sciences and Clinical Research (JSSCR)
Volume 8 Number 1, 2026
Journal Homepage: http://ejurnal.uniga.ac.id/index.php/jsscr, E-ISSN: 2656-9612 P-ISSN:2656-8187
DOI: http://dx.doi.org/10.37311/jsscr.v8i1.35343

Green-Synthesised AgNP–Chitosan Nanocomposites Using *Cymbopogon citratus* Extract: SEM, FTIR, and Tensile Characterisation

Komariah[1*], Jenifer Angela Gunawan[2], Florencia Livia[3], Rezky Anggraeni[4], Dewi Ranggaini[5], Johni Halim[6]

[1,4] *Department of Oral Biology, Faculty of Dentistry, subdivision Histology, Universitas Trisakti, Faculty of Dentistry, Trisakti University, Jl. Kyai Tapa No. 1 Grogol Petamburan, West Jakarta 11440, Indonesia*
[2] *Student Faculty of Dentistry, Universitas Trisakti, Jl. Kyai Tapa No. 1 Grogol Petamburan, West Jakarta 11440, Indonesia*
[3] *Department of Dental Materials, Faculty of Dentistry, Universitas Trisakti, Jl. Kyai Tapa No. 1 Grogol Petamburan, West Jakarta 11440, Indonesia*
[5,6] *Department of Oral Biology, Faculty of Dentistry, Subdivision Physiology, Universitas Trisakti, Jl. Kyai Tapa No. 1 Grogol Petamburan, West Jakarta 11440, Indonesia*

** Corresponding author. Email: komariah@trisakti.ac.id*

ABSTRACT

The development of nanomaterials in dentistry has brought significant innovations in improving the effectiveness of treatments, particularly in biomedical applications. One important implementation is the development of nanocomposites, which are composite materials consisting of nano-sized fillers and stabilizing agents. Silver nanoparticles (AgNP) obtained through green synthesis using lemongrass (*Cymbopogon citratus*) leaf extract tend to aggregate easily, therefore, a stabilizing agent in the form of chitosan is needed. This study aims to determine the physical and chemical characteristics of AgNP nanocomposites synthesized using *C. citratus* extract as a reducing agent and chitosan as a stabilizing agent. Physical characterization testing was performed using Scanning Electron Microscopy (SEM) and tensile strength testing. Chemical characterization was performed through Fourier Transform Infrared (FTIR) testing. SEM analysis revealed an asymmetrical morphology, featuring a dense layer and a relatively uniform dispersion of nanoparticles within the polymer matrix. The combination of chitosan and the extract maintained structural stability with only slight agglomeration in the nanometer range. Tensile strength testing revealed that the chitosan–AgNP membrane exhibited the highest tensile strength of 17.64 ± 0.001 MPa. The chitosan–AgNP membrane had an elongation of 6.03±0.001% and a stress at break of 17.64±0.001 MPa, which was higher than that of the other membrane groups. FTIR analysis identified hydroxyl (3416.17 cm^{-1}), amide (1640.15 cm^{-1}), and siloxane (1034.44 cm^{-1}) groups, confirming the integration of the organic and inorganic hybrid structure. XRD analysis revealed 12% crystallinity and a dominant amorphous phase of 88%. Conclusion: AgNP nanocomposite membranes synthesized with *C. citratus* extract and chitosan as a stabilizing agent exhibit good physical and chemical properties for biomedical applications. These properties include homogeneous particle distribution, adequate mechanical strength, a stable chemical structure, and optimal crystallinity for wound healing applications.

Licensed under: Creative Commons Attribution (CC-BY-SA)

Keywords:
Silver Nanoparticles; *Cymbopogon citratus*; Chitosan; Nanocomposites; FTIR; Tensile Properties

Received:	Accepted:	Online:
2025-11-15	2026-01-16	2026-01-25

1. Introduction

Nanotechnology has brought about significant transformations in various fields, including dentistry, where the development of nanocomposites has provided significant innovations to improve the effectiveness of treatments [1],[2]. Nanocomposites, as composite materials consisting of nanoparticle fillers on a scale of 1-100 nm, combined with a polymer matrix that functions as a stabilizing agent or capping agent, have the potential to produce new materials with superior properties compared to conventional materials [3],[4]. One of the most widely used fillers is silver nanoparticles (AgNP), which are known for their antibacterial activity and biocompatibility. The formation of silver nanoparticles (AgNPs) typically begins with silver nitrate ($AgNO_3$) as a precursor of Ag^+ ions. Although $AgNO_3$ is widely used for its antimicrobial properties, its direct application may raise concerns related to toxicity and environmental impact. To address these issues, lemongrass leaves (Cymbopogon citratus) are employed as a biological reducing agent, facilitating the reduction of Ag^+ to metallic Ag^0 under mild and environmentally friendly conditions [5].Lemongrass leaves contain various secondary metabolites, including alkaloids, flavonoids, saponins, tannins, essential oils, phenolic compounds, and other phytochemicals, which exhibit pharmacological activities such as anti-inflammatory, anti-obesity, antifungal, antinociceptive, antioxidant, and antibacterial effects [6]. These bioactive compounds act not only as natural reducing agents but also as stabilizing agents during AgNP synthesis, enabling control over particle size and morphology. The use of lemongrass leaf extract offers several advantages, including ease of availability, a green synthesis approach that minimizes the use of harsh chemical reagents, and reduced risk of excessive silver ion exposure, thereby enhancing the biocompatibility of the resulting nanoparticles [7],[8].

The silver nitrate reduction process converts Ag+ ions into Ag0, which then transforms into AgNP, a silver nanoparticle that acts as a filler or filling agent. AgNP has antimicrobial activity against several pathogenic microbes, such as bacteria, fungi, algae, and viruses [9],[10]. AgNP on a nano scale has better potential with maintainable size and stability. Previous studies have shown that lemongrass leaf extract has been successfully used as a bioreductor to produce relatively small and stable AgNP [7]. In general, AgNP has low stability and easily aggregates to form larger particles. Therefore, a stabilizing agent is needed to prevent aggregation between silver nanoparticle surfaces, namely chitosan [11].

Chitosan is a natural polymer resulting from the deacetylation of chitin, which can be obtained from the shells of crustaceans, such as crabs and shrimp [12]. It can also be obtained from insects, such as the horned beetle (*Xylotrupes gideon*) [12]. Horned beetles are considered pests because if their population becomes too large, they can damage coconut trees [12]. The use of *X. gideon* as a source of chitosan has significant advantages because its chitin content reaches 47%, which is much higher than other crustaceans such as shrimp and rajungan [13]. The high chitin content maKEs it a better choice in terms of utilization and efficiency in chitosan production because it can produce chitosan with superior physicochemical properties and biological activity, especially in biomedical applications [14].

AgNP nanocomposites capped with chitosan show significant potential for medical applications because they have antibacterial properties and help improve the

wound healing process [15]. Nanocomposites made with metal-based, non-metal-based, and polymer-based materials also provide excellent benefits such as surface deformation and other characteristics of the materials produced. With the addition of nanomaterials, the polymer can significantly improve its properties or produce new properties, depending on the type of nanomaterial used [16]. The combination of chitosan and AgNP provides an effective approach to treating infections, supporting tissue regeneration, and accelerating the wound healing process, both on the skin and in the oral cavity [17].

Good characteristics are determined by a combination of interacting physical and chemical properties. Physically, the results of Scanning Electron Microscopy (SEM) analysis show that the thickness of the nanocomposite affects its mechanical strength and separation efficiency [18]. Increased thickness strengthens the nanocomposite structure but tends to reduce flux [18]. Based on tensile strength testing, the ideal nanocomposite has high tensile strength, proportional elastic modulus, and adequate elongation [14],[19]. Chemically, Fourier Transform Infrared (FTIR) analysis identifies active functional groups through absorption at specific wavelengths related to the chemical properties of nanocomposites, such as hydrophilicity and surface interactions. [20].

Previous studies have shown that natural materials have great potential in the synthesis and modification of nanocomposites. Lemongrass leaf extract (*Cymbopogon nardus*) has been reported to act as a reducing agent and stabilizer for silver nanoparticles (AgNP) through the interaction of –OH and C=O groups, resulting in a crystalline structure with a particle size of approximately 8.40 nm [21]. Meanwhile, another study reported the successful synthesis of chitosan from shrimp shell waste as a base material for nanocomposite production, marKEd by the disappearance of amide groups in FTIR [22]. This study indicates that pure chitosan from shrimp shell waste is not yet effective enough to be applied as an antimicrobial agent [22].

Based on these studies, the present research focuses on modifying the nanocomposite synthesis system by integrating lemongrass (Cymbopogon citratus) leaf extract as a natural reducing agent and horned beetle–derived chitosan as a stabilizing (capping) agent to prevent aggregation among silver nanoparticle (AgNP) surfaces. This strategy is expected to yield a chitosan–Ag nanocomposite with improved chemical and physical stability, enhanced antimicrobial activity, and increased suitability for wound healing applications. Accordingly, this work aims to synthesize AgNP–chitosan nanocomposites using C. citratus leaf extract and to characterize their morphology using scanning electron microscopy (SEM), mechanical properties through tensile testing, and functional groups by Fourier transform infrared spectroscopy (FTIR).

2. Material and Methods

The research method used was descriptive experimental research. This study tested the physical and chemical characteristics of AgNP nanocomposites reduced with *C. citratus* extract and the use of chitosan as a stabilizing agent. The AgNPs were washed and centrifuged. The obtained precipitate was weighed and mixed with the chitosan solution. The following materials were used, 96% alcohol, distilled water, acetic acid, 2% (v/v), chitosan, NaOH, Tripolyphosphate (Sigma Aldrich), Tween 80 (Sigma Aldrich).

Preparation of Lemongrass Leaf Extract (*C. citratus*)

The lemongrass leaves used in this study were obtained from the Spice, Medicinal, and Aromatic Plant Instrument Standards Testing Center (BSIP-TROA) and

have been identified. Leaves that have been dried for one week will be powdered by reducing their size using a plant grinding machine [23]. Extraction was carried out using the maceration method, with lemongrass leaf powder soaKEd in 70% ethanol at a ratio of 1:10 for 24 hours [7]. The maceration process was carried out for 3 days, with manual stirring for 15 minutes every 8 hours to maintain the homogeneity of the solution. After maceration was complete, the solution was filtered using Whatman No. 1 filter paper to separate the pulp from the filtrate. The filtrate obtained was then evaporated using a rotary evaporator at a temperature of 50–60 °C to obtain a crude extract [24].

Preparation of AgNP Chitosan Nanocomposite

Lemongrass leaf extract is dissolved in 10 mL of water. Mix 10 mL of the extract solution with 90 mL of 0.1 M $AgNO_3$ solution, stir using a magnetic stirrer at a speed of 2000 rpm while heating at a temperature of 40°C. The mixture is incubated for 24 hours in dark conditions (wrapped in aluminum foil). After incubation, the mixture is washed with distilled water and centrifuged at a speed of 5000 rpm. The precipitate obtained is weighed at 0.25 mg and mixed in 5 mL of 1.5% chitosan solution (w/v), stirring the mixture for 30 minutes with a magnetic stirrer at a speed of 2500 rpm. Add the Add 0.1% tripolyphosphate solution drop by drop to the chitosan-AgNP mixture while continuing to stir, followed by the addition of 0.1% Tween 80 and stirring again. Measure the pH of the mixture. If it is too acidic, adjust it by adding 0.1 N NaOH drop by drop while stirring until the pH reaches 6.0–7.0. Pour the solution into a Petri dish at room temperature and let it stand for 48 hours. Carefully remove the chitosan-Ag membrane sample until the membrane is retrieved. Prepare the control group in the same manner, adding either 0.25 mg of extract (membrane-Ke), 0.25 mg of $AgNO_3$ (membrane-Ag), or chitosan only (membrane-Chi) (Table 1).

Table 1. Membrane composition

Group	Chitosan 1.5% (w/v)	AgNP	Extract	$AgNO_3$
Nanocomposite membrane $AgNO_3$ (KAg)	5 mL	-	-	0.25 mg
Nanocomposite membrane AgNP	5 mL	0.25 mg	-	-
Nanocomposite membrane chitosan	5 mL	-	-	-
Nanocomposite membrane extract	5 mL	-	0.25 mg	-

SEM Characterization Test

This SEM study was conducted using synthesized membrane samples. The samples were then coated with a conductive layer, such as gold, using a sputter coater to prevent charge accumulation on the sample surface. The samples were placed in a SEM vacuum chamber and analyzed using an electron beam to produce high-resolution images of the membrane surface. The images obtained were used to examine the surface morphology, distribution of AgNP nanoparticles, and interaction between AgNP and chitosan, as well as to evaluate the uniformity and quality of the resulting nanocomposite membrane [25].

Characterization Test: Tensile Strength

In this study, tensile strength testing was conducted by preparing nanocomposite membrane samples that had been cut into a standard dumbbell shape, referring to the ASTM method commonly used for testing thin materials [26]. The test samples were

mounted on a Shimadzu AGX 690 universal testing machine, with both ends of the membrane clamped symmetrically and firmly to the machine grip so that they would not shift during testing. The tensile test was conducted at a constant speed of 10 mm/minute [27]. During the test, the samples were slowly pulled by the machine until they were damaged or broken. The machine automatically recorded the maximum tensile force (kgF) and sample elongation (Δl) that occurred during the pulling process. The data obtained was in the form of max force and max stress, which were used to calculate tensile strength as the maximum force and stress before breaking, and to calculate stress at break as the stress at the moment the material failed. Max strain was used to calculate elongation or maximum strain until material failure occurred [26].

FTIR Characterization Test

The chitosan–Ag nanocomposite samples were cut into appropriate sizes and analyzed using Fourier transform infrared (FTIR) spectroscopy [28]. Measurements were performed in attenuated total reflectance (ATR) mode at room temperature, with spectra recorded over the wavenumber range of 4000–400 cm^{-1}, a spectral resolution of 4 cm^{-1}, and 32 scans averaged for each sample to improve the signal-to-noise ratio. Prior to analysis, baseline correction and atmospheric compensation were applied to all spectra. Infrared radiation absorbed by the chemical bonds within the chitosan–Ag nanocomposite generated characteristic absorption bands corresponding to molecular vibrational modes [15]. The obtained spectra were analyzed to identify functional groups, chemical composition, and intermolecular interactions between chitosan and silver nanoparticles by comparison with reference spectra and FTIR databases. In addition, FTIR spectra of control samples, including pure chitosan, $AgNO_3$, lemongrass leaf extract, and chitosan-only membranes, were recorded under identical conditions to support accurate band assignment and interpretation.

Data Analysis

Data from physical and chemical characteristic tests, including SEM testing, tensile strength testing, and FTIR testing, were analyzed and compared with standards set by the International Organization for Standardization (ISO), ensuring that chitosan nanocomposites -Ag nanocomposite has high mechanical strength and resistance to tensile loads, a homogeneous surface structure and even pore distribution, strong chemical stability and composition, and a consistent crystal structure to meet performance, durability, and safety requirements, especially for biomedical applications.

3. Results and Discussion

SEM Characterization

Based on the conducted research, the chitosan–Ag nanocomposites synthesized using *Cymbopogon citratus* extract with chitosan as a stabilizing agent exhibited morphological features that suggest the formation of an asymmetric nanocomposite structure, characterized by a relatively compact upper surface and a more porous underlying region. These features were observed from surface topographical SEM images recorded at various magnifications (**Figure 1**). At low magnification (×500), the nanocomposite surface showed the presence of micrometer-scale aggregates with sizes ranging from approximately 5–15 µm, distributed within a smooth and homogeneous background. These structures are interpreted as secondary aggregates composed of smaller particles, while the surrounding smooth regions indicate that the chitosan polymer network is well formed and uniformly covers the nanocomposite surface. Increasing the magnification to ×1000 revealed that these aggregates exhibited a globular

to semi-spherical morphology with dominant sizes of 3–10 µm, randomly yet relatively evenly distributed across the surface. This distribution suggests effective interactions between the nanoparticle domains and the functional groups of chitosan, potentially enhanced by bioactive compounds present in the *C. citratus* extract acting as natural stabilizing agents.

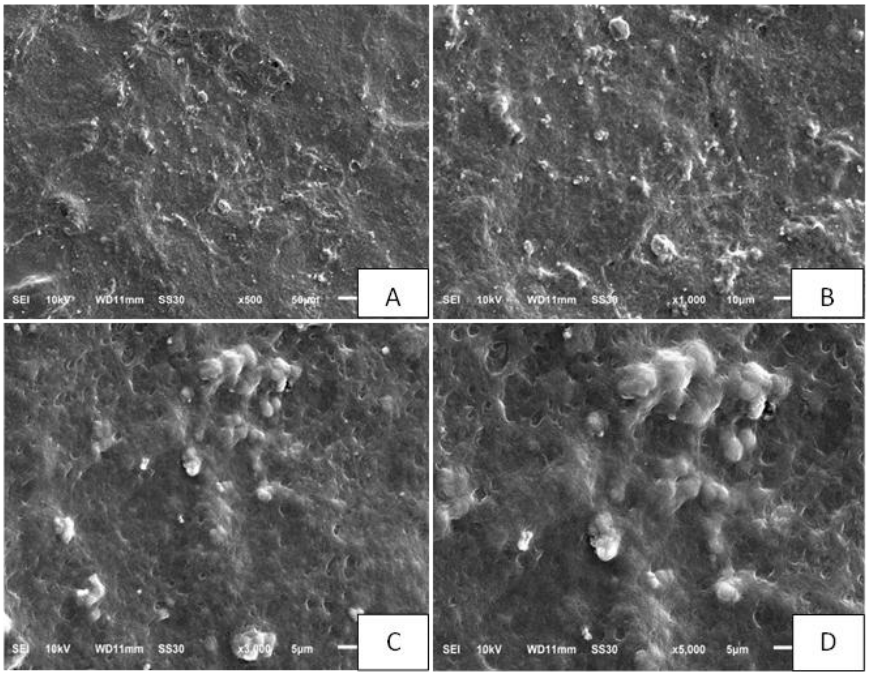

Figure 1. SEM characterization results with magnifications of x500 (A), x1000 (B), x3000 (C), and x5000 (D)

At higher magnification (×3000), the microstructure consisted of compact clusters formed from submicron- to micrometer-sized particles, indicating aggregation driven by intermolecular forces such as van der Waals interactions and electrostatic attraction between chitosan-coated domains. At the highest magnification (×5000), primary nanoparticle domains with an estimated size range of 50–200 nm were observed, which are considered the fundamental building blocks of the larger aggregates. These nanoscale domains appeared to be embedded within and coated by the chitosan matrix and organic compounds derived from the lemongrass extract.

Regions with higher brightness contrast in the SEM images may correspond to areas enriched with silver-containing phases; however, the presence and spatial distribution of silver cannot be conclusively determined based on SEM contrast alone. Therefore, complementary elemental analysis, such as energy-dispersive X-ray spectroscopy (EDS/EDX) mapping, is required to confirm the distribution of Ag within the nanocomposite matrix.

Overall, the observed morphology indicates a generally good level of nanoparticle dispersion, although localized fine agglomeration remains in certain areas. These observations suggest that interactions between AgNP domains, chitosan functional groups (–NH_2 and –OH), and bioactive compounds from C. citratus extract contribute to the formation of a balanced organic–inorganic hybrid system with enhanced structural stability. The formation of primary nanoparticle domains within the 50–200 nm size range indicates that the silver ion reduction process was effective;

however, cross-sectional SEM analysis is necessary to conclusively verify the asymmetric architecture and to clarify whether the observed morphology arises from a phase-inversion mechanism during membrane casting.

Previous studies have reported that biogenically synthesized silver–chitosan nanocomposites exhibit smooth surfaces, relatively uniform particle distribution, and enhanced stability due to the encapsulation of silver particles by chitosan [29]. Other reports have described asymmetric morphologies in polymer-based nanocomposites, typically consisting of a dense upper layer and a porous sublayer associated with phase-inversion membrane formation and improved mechanical performance [30]. The morphological features observed in the present study are consistent with these reports, while further confirmation using EDS elemental mapping and cross-sectional SEM imaging is recommended to strengthen the interpretation of nanoparticle distribution and structural asymmetry.

Tensile Strength Characterization

The results of testing the characteristics of AgNP nanocomposite membranes with C. citratus extract and chitosan as stabilizing agents using a Universal Testing Machine (UTM) showed the performance of each membrane in terms of tensile strength, stress at break, and elongation. This test covered four different groups of membranes. The tensile strength test results using UTM from the test and control groups can be seen in **Table 2**.

Table 2. Tensile strength on nanocomposites

Parameters	**Group**				
	Nanocomposite membrane $AgNO_3$ (KAg)	Nanocomposite membrane AgNP	Nanocomposite membrane chitosan	Nanocomposite membrane extract	*p Value*
Tensile Strength (MPa)	6.85± 0.001[d]	17.6.4± 0.001[a]	9.95± 00.01[c]	11.28± 0.001[b]	$p < 0.01$
Stress at Break (MPa)	6.85± 0.001[d]	17.64± 0.001[a]	9.95± 0.001[c]	11.28± 0.001[b]	
Elongation (%)	5.18± 0.001[c]	603± 0.001[a]	4.26± 0.001[d]	5.66± 0.001[b]	

The tensile strength test results show that there are significant differences between the test groups, which consist of AgNP membranes, KAg membranes, K membranes, and Ke membranes, with the highest tensile strength occurring in KAg membranes, followed by Ke membranes, K membranes, and AgNP membranes. The stress at break test results showed that there were significant differences between all test groups, with the highest stress at break value occurring in the KAg membrane, followed by the Ke membrane, K membrane, and AgNP membrane. The elongation test results also showed significant differences between the test groups, with the highest elongation value occurring in the KAg membrane, followed by the Ke membrane, AgNP membrane, and K membrane.

In the tensile strength test, the membrane groups showed a significant difference ($p < 0.001$). The highest value was obtained by the chitosan–AgNP membrane at 17.64

MPa, which was significantly higher than the value obtained by the AgNP membrane at 6.85 MPa. This increase indicates the dominant role of the chitosan matrix as a continuous polymer phase that can effectively transfer loads while the silver nanoparticles function as reinforcements dispersed in the matrix. In chitosan-AgNP membranes, interfacial interactions in the form of hydrogen bonds and coordination between the -NH_2 and -OH groups of the chitosan and the surface of the AgNPs produce a more homogeneous and compact composite structure. This results in a more even stress distribution [31],[32]. In AgNP membranes without an adequate chitosan matrix, the distribution of the nanoparticles tends to be suboptimal, forming stress concentration points. This results in a lower tensile load-bearing capacity. The same pattern was observed in the stress-at-break value: the chitosan-AgNP membrane showed the highest value at 17.64 MPa, compared to 6.85 MPa for the AgNP membrane. These results confirm that the chitosan-AgNP composite structure is more resistant to mechanical failure due to structural reinforcement and stable interfacial bonds.

In terms of elongation, the chitosan–AgNP membrane exhibited a higher value of 6.03%, compared to 4.26% for the pure chitosan membrane. This indicates an increased deformation capacity without a loss of mechanical strength. The pure chitosan membrane's low elongation value is related to its relatively brittle matrix properties, which are due to the dominance of intramolecular hydrogen bonds that limit polymer chain mobility. Adding AgNPs to the chitosan–AgNP membrane increased the material's flexibility, allowing for greater deformation before breaking. Combining chitosan and AgNPs increased tensile strength and produced an optimal balance of stiffness and flexibility in the membrane. Previous studies have shown that adding glycerol plasticizer to acetate cellulose membranes increases flexibility but decreases tensile strength due to reduced polymer chain interactions. These results differ from those of this study because the developed nanocomposite membranes exhibit strong tensile strength and good mechanical stability without the use of plasticizers.

FTIR Characterization

The FTIR analysis of the AgNP nanocomposites synthesized using Cymbopogon citratus extract and chitosan as a stabilizing agent revealed the presence of characteristic functional groups associated with an organic–inorganic hybrid system dominated by the chitosan matrix and plant-derived compounds. The observed functional groups primarily include hydroxyl (–OH), amine (–NH_2/–NH), and polysaccharide-related oxygen-containing groups, which are indicative of successful nanocomposite formation. A broad absorption band centered at 3416.17 cm^{-1} was assigned to overlapping –OH stretching vibrations and –NH stretching modes, originating from hydroxyl groups in chitosan and phenolic compounds in the *C. citratus* extract, as well as amine groups of chitosan. The broad nature of this band suggests the presence of intermolecular hydrogen bonding, indicating interactions between the chitosan matrix, bioactive compounds, and silver nanoparticle domains (**Figure 2**).

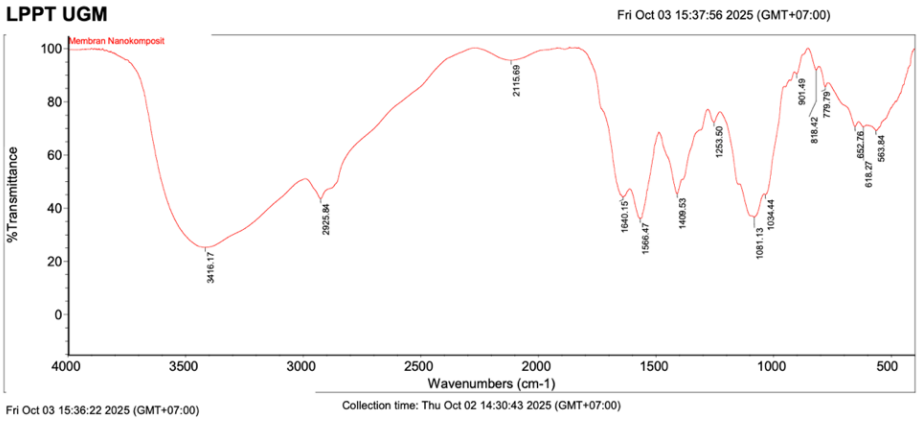

Figure 2. FTIR characterization results

Absorption bands in the region of 1034.44–1081.13 cm^{-1} are attributed to C–O and C–O–C stretching vibrations of the polysaccharide backbone of chitosan, which are characteristic of glycosidic linkages in chitosan and other polysaccharides. These peaks may also include contributions from oxygenated functional groups present in the C. citratus extract. Importantly, these bands are not assigned to siloxane (Si–O–Si) groups, as no silica- or silicate-based fillers were incorporated in the nanocomposite system. Characteristic amide bands of chitosan were observed at 1640.15 cm^{-1}, corresponding to C=O stretching vibrations of amide I, and at 1566.47 cm^{-1}, associated with N–H bending and C–N stretching of amide II. The presence and slight shifts or intensity changes of these bands relative to control samples (pure chitosan and chitosan–extract systems) suggest interactions between chitosan functional groups (–NH_2 and –OH) and AgNP domains, potentially through coordination interactions and hydrogen bonding. The absorption band at 2925.84 cm^{-1} was assigned to the asymmetric stretching vibration of –CH_2 groups, confirming the presence of aliphatic hydrocarbon chains within the chitosan backbone and contributing to the flexibility of the nanocomposite. A band at 1409.53 cm^{-1} corresponds to –CH_3 bending vibrations, further supporting the presence of organic polymer chains.

The fingerprint region between 563.84 and 901.49 cm^{-1} exhibited multiple absorption features that may be associated with out-of-plane bending vibrations of substituted organic groups and metal–oxygen interactions related to Ag–O bonding. However, these assignments remain indicative and require further confirmation through complementary techniques such as EDS or XRD analysis. Overall, the FTIR results demonstrate the successful integration of chitosan, *C. citratus* extract, and silver nanoparticle domains within the nanocomposite matrix. The interpretation is based on qualitative and relative spectral changes compared to control samples, rather than absolute intensity values, due to the absence of a calibration model. These findings support the role of chitosan functional groups in stabilizing AgNPs and forming a cohesive organic–inorganic hybrid system.

The integration of *C. citratus* extract acts as a stabilizing and structural reinforcing agent that supports the formation of a compact and homogeneous polymer network. Chemically, the presence of AgNP and bioactive compounds from the extract forms cross-linking that strengthens the polymer matrix, reduces solubility due to polar hydroxyl groups, and increases resistance to solvents and acidic environmental conditions. The complex interaction between the -NH_2 groups of chitosan, AgNP, and

C. citratus extract results in a more consolidated network configuration with high structural integrity. The resulting chitosan-Ag nanocomposite is not easily soluble in conventional polar solvents but retains its ampholytic properties and sensitivity to changes in environmental pH. Under oral cavity pH conditions approaching neutrality, this chitosan-Ag nanocomposite can undergo partial softening without losing its mechanical stability, demonstrating adaptive characteristics suitable for biomedical applications.

This study has several limitations that should be noted. The distribution and identity of AgNPs were mainly inferred from surface SEM observations and FTIR analysis; thus, elemental mapping (EDS/EDX) and cross-sectional SEM are needed to confirm silver localization and structural asymmetry. Moreover, the interactions among chitosan, AgNPs, and C. citratus extract were interpreted qualitatively. Further validation using techniques like XPS or long-term stability and silver release studies is necessary. Finally, the performance of the nanocomposite was tested in a lab setting, which may not fully represent the changing environment of the mouth.

4. Conclusion

This work concludes that AgNP–chitosan nanocomposites prepared through *Cymbopogon citratus* extract have an asymmetric surface morphology, consisting of micrometer-size clusters and primary nanoparticles in the range 50–200 nm at magnification (×5000), observed from SEM analysis. The stabilization of chitosan as stabilizing agent leads to dispersion of the nanoparticles in the polymer matrix while avoiding excessive aggregation. The FTIR analysis degree also supported the presence of hydroxyl and amine functional groups related to chitosan (and plant compounds) that were engaged in the formation of nanoparticles and interphase interactions. If the chemical compound, crysta l structure and bulk mechanical behavior were similar though, that was not the case for ele mental composition.

Acknowledgements:
The authors would like to express their deepest gratitude to all parties who contributed to the completion of this research.

Conflicts of Interest:
The author declares that there are no conflicts of interest related to the publication of this journal.

References

[1] AlKahtani, Rawan N. "The Implications and Applications of Nanotechnology in Dentistry: A Review." The Saudi Dental Journal. 2018; 30(2): 107-116. Available: https://doi.org/10.1016/j.sdentj.2018.01.002.

[2] Aini, D. M., Antari, G. Y., Ratnasari, B. D. "Herbal Nanoparticles: The Advantages of Ginger and Gotu Kola for the Immune System." Nuansa Fajar Cemerlang. 2025. Available: https://repository.nuansafajarcemerlang.com/publications/591591/nanopartikel-herbal-keunggulan-jahe-dan-pegagan-untuk-sistem-imun

[3] Ady, J., Aziz, M. A., & Seha, S. N. "Synthesis of SiO2 – PVA – Gelatine Nanocomposite Membrane by Handling of the Gelatine." Journal of Physics: Conference Series. 2020; 1445(1): 1–7. Available: https://doi.org/10.1088/1742-6596/1445/1/012016.

[4] Huq, M. A., Hasan, M. M., & Hossen, M. I. "Green Synthesis and Potential Antibacterial Applications of Bioactive Silver Nanoparticles: A Review." Polymers. 2022;14(4):742. Available: https://doi.org/10.3390/polym14040742.

[5] Amri, I. A., Hendrasmara, M. F., Qosimah, D., Aeka, A., Rickyawan, N., Purwatiningsih, W., et al. "Toxicity of Silver Nitrate ($AgNO_3$) Solution in BALB/c Mice Based on SGPT and SGOT Levels." Jurnal Medik Veteriner. 2020; 3(2): 251–257. Available: https://doi.org/10.20473/jmv.vol3.iss2.2020.251-257.

[6] Cortes-Torres, A. G., López-Castillo, G. N., Marín-Torres, J. L., Portillo-Reyes, R., Luna, F., Baca, B. E., et al. "*Cymbopogon citratus* Essential Oil: Extraction, GC–MS, Phytochemical Analysis, Antioxidant Activity, and In Silico Molecular Docking for Protein Targets Related to CNS." Current Issues in Molecular Biology. 2023; 45(6): 5164–5179. Available: https://doi.org/10.3390/cimb45060328.

[7] Rifai, S. Q. Y., Rante, H. "Green Synthesis of Silver Nanoparticles (AgNPs) Using Lemongrass (Cymbopogon citratus) Leaf Extract as a Bioreducing Agent." Majalah Farmasi Farmakologi Fakultas Farmasi Makassar. Available: https://journal.unhas.ac.id/index.php/mff/article/view/21047/9122.

[8] Siampa, J. P., Tiku, J. F., Fatmawaty, A., Arjuna, A. "Production of Silver Nanoparticles Using *Curculigo orchioides* Rhizome Infusion as a Bioreductor: Effects of $AgNO_3$ Concentration and Reduction Time." Majalah Farmasi Farmakologi. 2020; 24(3): 93–97. Available: https://doi.org/10.20956/mff.v24i3.11965

[9] Jeevanandam, J., Krishnan, S., Hii, Y. S., Pan, S., Chan, Y. S., Acquah, C., et al. "Synthesis Approach-Dependent Antiviral Properties of Silver Nanoparticles and Nanocomposites." Journal of Nanostructure in Chemistry. 2022; 12(5): 809–831. Available: https://doi.org/10.1007/s40097-021-00465-y.

[10] Mohanta, Y., Nayak, D., Biswas, K., Singdevsachan, S., Abd_Allah, E., Hashem, A., et al. "Silver Nanoparticles Synthesized Using Wild Mushroom Show Potential Antimicrobial Activities against Food Borne Pathogens." Molecules, 2018; 23(3): 1–18. Available: https://doi.org/10.3390/molecules23030655.

[11] Az Zahra, U. F., Hindryawati, N., Panggabean, S. A. "Synthesis and Characterization of Chitosan-Modified Silver Nanoparticles Using $NaBH_4$ as a Reducing Agent." Jurnal Atomik. 2024; 9(2): 120–127. Available: https://doi.org/10.30872/ja.v9i2.1406.

[12] Livia, F., Tjandrawinata, R., Marpaung, C. D., Pratiwi, D., & Komariah, K. "The Effect of Horn Beetle Nano Chitosan (Xylotrupes Gideon) on the Surface Roughness of Glass-Ionomer Cement." Materials Science Forum. 2022; 1069: 161–166. Available: https://doi.org/10.4028/p-5mk858.

[13] Pratiwi, D., Salim, R. F., Tjandrawinata, R., Komariah, K. "Surface Morphology Evaluation of Glass Ionomer Cement Modified with Rhinoceros Beetle Nanochitosan." Jurnal Kedokteran Gigi Universitas Padjadjaran. 2021; 33(3): 240–246. Available: https://doi.org/10.24198/jkg.v33i3.32231

[14] S, M., N, R., & Ramu, R. "Chitosan and Oral Mucosal Wound Healing in Dentistry—Journey from Non-Patented to Patent Introspection from 2010–202." Journal of Applied Pharmaceutical Science. 2020; 12(4): 12–25. Available: https://doi.org/10.7324/JAPS.2022.120402.

[15] Notriawan, D., Nesbah, N., Ernis, G., Fadhila, M. A., Wibowo, R. H., Pertiwi, R., et al. "Antibacterial Activity of Chitosan/Silver Nanoparticle Nanocomposites." ALCHEMY. 2021; 9(1): 26–31. Available: https://doi.org/10.18860/al.v9i1.11146

[16] C, Pavan, and Madhavi Blr. "Nanocomposites: - A Recent Overview." Global Journal of Medical Research. 2020; 20(7): 9–21. Available: https://doi.org/10.34257/GJMRBVOL20IS7PG9.

[17] Chicea, D., Nicolae-Maranciuc, A., & Chicea, L. "Silver Nanoparticles-Chitosan Nanocomposites: A Comparative Study Regarding Different Chemical Syntheses Procedures and Their Antibacterial Effect." Materials. 2024; 17(5): 1–22. Available: https://doi.org/10.3390/ma17051113.

[18] Bhernama, B. G., Nurhayati, N., Saputra, S. A., & Amalia, N. J. "Characterization of Cellulose Acetate Nanokomposite from Nutmeg Shells." Sains Natural: Journal of Biology and Chemistry. 2023; 13(3): 152–160. Available: https://doi.org/10.31938/jsn.v13i3.465.

[19] Liu, S., Li, D., Yang, Y., & Jiang, L "Fabrication, Mechanical Properties and Failure Mechanism of Random and Aligned Nanofiber Nanokomposite with Different Parameters." *Nanotechnology Reviews*. 2019; 8(1): 218–26. Available: https://doi.org/10.1515/ntrev-2019-0020.

[20] Zulnazri, Z., Lestari, D., Hakim, L., Dewi, R., Sulhatun, S. "Study on Cellulose Extraction from Areca Nut Husk Using NaOH Solution." Jurnal Teknologi Kimia Unimal. 2022; 11(2): 193–206. Available: https://doi.org/10.29103/jtku.v11i2.7846.

[21] Kamarudin, N. S., Jusoh, R., Setiabudi, H. D., Jusoh, N. W. C., Jaafar, N. F., & Sukor, N. F. "Cymbopogon Nardus Mediated Synthesis of Ag Nanoparticles for the Photocatalytic Degradation of 2,4-Dicholorophenoxyacetic Acid." Bulletin of Chemical Reaction Engineering & Catalysis. 2019; 14(1): 173–181. Available: https://doi.org/10.9767/bcrec.14.1.3321.173-181.

[22] Aldila, H., Swandi, M. K., & Dalimunthe, D. Y. "Synthesis and Antibacterial Activity of Chitosan Nanokomposite from Shrimp Shell Waste." IOP Conference Series: Earth and Environmental Science. 2021; 926(1): 1–8. Available: https://doi.org/10.1088/1755-1315/926/1/012016.

[23] Felicia F, Komariah K, Kusuma I. "Antioxidant Potential of Lemongrass (Cymbopogon citratus) Leaf Ethanol Extract in HSC-3 Cancer Cell Line." Trop J Nat Prod Res. 2022; 6(4): 520-528. Available: https://doi.org/10.26538/tjnpr/v6i4.10.

[24] Fitria, N., Bustami, D. A., Komariah, K., & Kusuma, I. "The Antioxidant Activity of Lemongrass Leaves Extract against Fibroblasts Oxidative Stress." Brazilian Dental Science. 2022; 25(4): 1–11. Available: https://doi.org/10.4322/bds.2022.e3434.

[25] Yahya, N. F. D., Sinala, S., Stevani, H. "Improvement of Ketoprofen Solubility in Microparticle Form Using the Emulsification–Ionic Gelation Method with Polyvinylpyrrolidone (PVP) and Tripolyphosphate (TPP)." Media Farmasi. 2024; 20(2): 257–263. Available: https://doi.org/10.32382/mf.v20i2.1006.

[26] Beliu, H. N., Pell, Y. M., Jasron, J. U. "Analysis of Tensile and Bending Strength of Widuri–Polyester Composites." LONTAR Jurnal Teknik Mesin Undana. 2016; 3(2): 11–20. Available: https://doi.org/10.1234/ljtmu.v3i2.471.

[27] Bahtiar, A. D. M. "Tensile Strength Analysis of Kreco Chitosan Nanocomposites for Household Drinking Water Filtration." Jurnal Mesin Nusantara. 2021; 4(2): 70–75. Available: https://doi.org/10.29407/jmn.v4i2.16789.

[28] Lestari, K. "Synthesis of Nanocomposite Materials." Universitas Nasional Press. 2021. Available: https://repository.unas.ac.id/id/eprint/3977.

[29] Mayeen, A., Shaji, L. K., Nair, A. K., & Kalarikkal, N. "Morphological characterization of nanomaterials." In *Elsevier eBooks*. 2018: 335–364. Available: https://doi.org/10.1016/b978-0-08-101973-3.00012-2

[30] Lubis, M. R. "Preparation and Characterization of Polyethersulfone (PES)–Chitosan Nanocomposites via Polymer Blending." Proceedings of the National Seminar, Politeknik Negeri Lhokseumawe. 2019; 3(1): 62–66. Available: http://e-jurnal.pnl.ac.id/semnaspnl/article/download/1711/1484

[31] Martínez-Cisterna, D., Chen, L., Bardehle, L., Hermosilla, E., Tortella, G., Chacón-Fuentes, M., et al. "Chitosan-Coated Silver Nanocomposites: Biosynthesis, Mechanical Properties, and Ag^+ Release in Liquid and Biofilm Forms." International Journal of Molecular Sciences. 2025; 26(9): 4130. Available: https://doi.org/10.3390/ijms26094130.

[32] Gaspar, A. L., Gaspar, A. B., Contini, L. R. F., Silva, M. F., Chagas, E. G. L., Bahú, J. O., et al. "Lemongrass (Cymbopogon citratus)-Incorporated Chitosan Bioactive Films for Potential Skincare Applications." International Journal of Pharmaceutics. 2022; 628: 122301. Available: https://doi.org/10.1016/j.ijpharm.2022.122301.